POLARIZED EFFECTS IN La DOPED $TlInS_2$ LAYERED SEMICONDUCTOR-II: POLARIZATION SWITCHING IN UNDOPED AND La - DOPED $TlInS_2$ FERROELECTRIC - SEMICONDUCTORS

M.Yu. SEYIDOV[1, 2], F.A. MIKAILZADE[1, 2], V.B. ALIYEVA[2], T.G. MAMMADOV[2], G.M. SHARIFOV[2], V.P. ALIYEV[2]

[1] Department of Physics, Gebze Technical University, 41400, Gebze, Kocaeli, Turkey
[2] Institute of Physics Azerbaijan National Academy of Sciences, AZ - 1143 Baku, Azerbaijan

Dielectric hysteresis loops of pure and lanthanum doped $TlInS_2$ ferroelectric – semiconductors were studied at the frequency 50 Hz for different temperatures below the Curie temperature (T_c). It has been revealed that, without any poling procedure, pure $TlInS_2$ exhibits normal single hysteresis loops at $T < T_c$. After electric field - cooled treatment of $TlInS_2$ the shape of hysteresis loops was strongly affected by corresponding charged deep level defects which were previously activated during the poling process. As a result, an additional defect polarization state from space charges accumulated on the intrinsic deep level defects has been revealed in pure $TlInS_2$ at the temperatures belowT_c. Besides, unusual multiple hysteresis loops were observed in La doped $TlInS_2$ at $T < T_c$ after application of different external perturbations (electric field, exposition and memory effect) to the sample. Measurements of the hysteresis loops in $TlInS_2$:La revealed the slim single, double and even triple polarization – electric field ($P – E$) hysteresis loops. This intriguing phenomenon is attributed to the domain pinning by photo – and electrically active La – impurity centers. The temperature variation of double - hysteresis loop was also investigated. Due to the heat elimination of the random local defect polar moments, the double – hysteresis loops were transformed into a normal single hysteresis loops on increasing the temperature.

Keywords: ferroelectric phase transitions; incommensurate phase; dielectric hysteresis loops; double dielectric loops.
PACS: 77.22.-d**;**77.22. Ej;77.70.+a; 77.80.-e

*Corresponding author. Address: Department of Physics, Gebze Technical University, Gebze, 41400, Kocaeli, Turkey. Tel.: +90 262 605 1329; fax: +90 262 653 8490
E-mail address: ***smirhasan@gtu.edu.tr*** (M-H.Yu.Seyidov).

1. INTRODUCTION

In a broad family of ferroelectric crystals, which possess spontaneous polarization reoriented by the electric field [1, 2], there is one which has played an especially important role in the physics of ferroelectricity in general. It is the ternary thallium indium disulphide - $TlInS_2$, the ferroelectric – semiconductor crystal with layered structure with monoclinic space group C_{2h}^6 at room temperature. The intensive research of various physical properties of this crystal during the past recent 40 years has led to an understanding of the mechanism of structural phase transitions in the materials which contain ferroelectric and semiconductor properties simultaneously as well as to new ideas related with the combination of the two branches: semiconductor physics and ferroelectricity (see Ref. [3 - 8] and references therein).

$TlInS_2$ is a well-known $\boldsymbol{p}$ - type semiconductor crystal [9, 10]. Its indirect and direct band gaps at 300K are: ~ 2.26 eV and ~ 2.34 eV correspondingly [11]. It has a high photoconductivity [12] in the visible range of light. The semiconductor characteristics of $TlInS_2$ single crystals studied by using optical and electrical measurements have been explained details in the literature. Additionally, the results of thermally stimulated current, photoluminescence and thermoluminescence investigations of $TlInS_2$ have been also presented recently in numerous works [13].

It has been revealed that, on cooling $TlInS_2$ undergoes structural phase transition (PT) from a paraelectric phase to incommensurably modulated phase at the temperature T_i ~ 216K. On further cooling, the wave vector of the incommensurate modulation changes until it locks into a commensurate wave vector at the Curie temperature T_c ~ 200K, and the structure transforms to a commensurate ferroelectric one [3 - 8]. In spite of a great number of studies, generally there isn't a clear picture for understanding the structure and origin of ferroelectricity in $TlInS_2$ at the temperatures below T_c.

Generally, ferroelectrics are known as insulating materials. The switchable electric polarization of these materials generally arises from a polar structural distortion of a high - symmetry reference structure. The ternary thallium chalcogenides $TlInS_2$ and $TlGaSe_2$ are ferroelectric - semiconductors with the same layered structure which undergoes phase transitions on decreasing the temperature from a high - temperature paraelectric phase to a low - temperature ferroelectric phase passing through an intermediate incommensurate phase. These ferroelectric – semiconductors have optical band - gap in the visible range and therefore have advantages of over other conventional ferroelectric materials. The possibility of electric field control of optical and electronic properties of $TlInS_2$ and $TlGaSe_2$ via the switchable polarization is of particular interest. For example, in a doped $TlInS_2$ ferroelectric - semiconductor, the polarization originated from a polar structural distortion can couple with internal electric field of charged deep – level defects. So, application of the electric field can be used directly to manipulate the electric polarization of $TlInS_2$ ferroelectric – semiconductor and thus control any semiconductor properties of $TlInS_2$ that are coupled to the polarization. This can give rise to multiple polarization states, switchable diode effect and bulk photovoltaic effect in which absorption of light by $TlInS_2$ material generates an asymmetric carrier distribution resulting in photocurrent.

131 H.Javid ave, AZ-1143, Baku
ANAS, G.M.Abdullayev Institute of Physics
E-mail: jophphysics@gmail.com

All these effects can lead to further technological applications of $TlInS_2$ improper ferroelectric – semiconductor in nonvolatile information storage, energy conversion and optoelectronics.

In recent years, several investigations have been performed for studying the relationship between ferroelectric domain walls and charged deep level defects in ferroelectric – semiconductors [5, 14 - 19]. It has been suggested that the polarization switching in ferroelectrics – semiconductors is strongly affected by the presence of charged deep level defects. Intrinsic defects in $TlInS_2$ have been the subject of intense investigation recently. In [16 - 20] photo - induced current transient spectroscopy (PICTS) has been applied to get more insight into spectra of intrinsic defects in high - resistive undoped $TlInS_2$ and La doped $TlInS_2$ crystals. Several deep level traps in wide band gap of undoped $TlInS_2$ and $TlInS_2$:La were obtained from transient properties of charge induced by photo – excitations [16 - 20]. In this paper, the important role of native charged deep level defects on the polarization switching properties of undoped $TlInS_2$ and $TlInS_2$: La was investigated through ferroelectric hysteresis loops measurements.

Lanthanum has been known as a kind of the photo - and electrically - active type of rare earth impurity center in semiconductor materials. Depending on the experimental conditions, La – dopant can be spontaneously ionized. In our previous works the change of dielectric properties of $TlInS_2$ induced by lanthanum dopant has been extensively studied [5, 14, 21]. Strong variations of the dielectric permittivity (ε) of $TlInS_2$: La within incommensurate (INC) phase has been found from measurements under external perturbations: the bias electric field and photoactive illumination. It has been obtained that the shape of the $\Delta\varepsilon(T)/\varepsilon(T)$ curves (here $\Delta\varepsilon$ is the difference between dielectric permittivity values measured under an external bias electric field and without it, and $\varepsilon(T)$ is the reference curve for $TlInS_2$: La without external perturbations) looks like the deviations of dielectric permittivity related with the memory effects observed inside INC - phase of undoped $TlInS_2$ crystal [5, 14, 21].

Note that the memory effect (ME) - "memorizing" the prehistory of a sample is the main characteristic of the INC - modulated systems A memory effect in incommensurate phases has been investigated in insulating materials and some charge – density wave compounds [22 - 26]. It has been revealed that after annealing for several hours at an annealing temperature T_{ann} within the INC - phase, the sample exhibits different physical properties from those in a non - annealed sample. The most remarkable property of the memory effect is that an incommensurate wave vector is unchangeable in several degrees around T_{ann} in heating and subsequent cooling processes.

Generally, this effect is caused by formation of defect density wave (DDW) as a result of rearranging of mobile defects on annealing of the crystal within INC - phase. The interaction between mobile defects included in a sample and INC - modulation gives rise to an ordered pattern of defects that is the frozen DDW. When the defects are mobile and the modulation is static, the diffusion of the defects occurs. The frozen DDW can seriously pin the INC – modulation of structure [22 - 26]. When the modulation is pinned by defects which are randomly distributed along its direction, the formation of metastable states as well as the existence of plateaus in the temperature dependence of the modulation wave vector and some other physical parameters can be revealed.

ME appears as a kink in the temperature dependence of the permittivity when the crystal is kept at the temperature within the INC phase during several hours. The usual temperature behavior of the permittivity is recovered on heating away from the annealing temperature. An inflection point of the kink is centered at an annealing temperature in the permittivity curve. Since the relaxation time of the mobile defects determined by their diffusion mobility considerably exceeds the time required for the measurements, it is possible to "conserve" the DDW in the temperature region outside the INC phase. If the sample is cooled below T_{ann} the DDW is pinned to the modulation wave on subsequent heating at T_{ann}, and this effect is called ME.

However, it is no unambiguous theoretical description of ME phenomenon existing in $TlInS_2$ in the frame of the general model. Recently we extended the DDW model and proposed a more complex model of charged intrinsic impurities interacting with INC wave in $TlInS_2$ [5, 14, 21]. In other words, the self - polarized DDW in $TlInS_2$ (and in $TlGaSe_2$ also) is created by charged defects leading to the internal bias field that can affect the all physical properties of crystal greatly [5, 14, 21].

Thus, another purpose of this work was to investigate the presence of the ME on ferroelectric hysteresis loops in $TlInS_2$:La. Additionally, we report the effect of the illumination of crystal by photoactive light with various wavelengths on P - E dependences in $TlInS_2$: La. A further was to study the influence of preliminary application of ***dc*** electric field to the crystal during cooling at different temperature ranges on P - E dependence of $TlInS_2$: La was also the aim of this work.

2. EXPERIMENTAL PROCEDURE

The technology of $TlInS_2$ crystals is presently developed well enough and its application does not possess great difficulties [9, 10]. The crystals of best quality are produced when combining crystal synthesis and growth processes within a single technological cycle. Polycrystalline $TlInS_2$ was synthesized from high purity (at least 99.999%) elements taken in stoichiometric proportions by chemical reaction in quartz ampoules. Normally, the synthesis of ~ 40 gr. of $TlInS_2$ compound takes place during 6 – 8 hours. Single crystals of $TlInS_2$ were grown using Bridgman – Stockbarger method from the melt of the starting materials sealed in evacuated ~ 10^{-5} Torr silica tubes with a tip at the bottom without any intentional doping. Single crystal growing was realized by slow melt crystallization technique using directional motion of sharp temperature gradient with the amount of 15K per millimetre in the vertical resistance furnace. Silica - glass tube with polycrystalline $TlInS_2$ was annealed above the melting point (~ 1035K) of the $TlInS_2$ compounds at about 5 – 10K and held at this

temperature for 2 - 3 days. The melt is mixed by vibration to gain homogeneity and intensify reacting parent substances. After this treatment the melt was moved from the hot side of zone furnace at ~ 1035K to the cold side at ~ 673K at the speed of 0.1 mm/h. In the cold zone, the crystal cooled down slowly within 2 – 3 weeks. The obtained crystal has a layered structure with glossy orange color and was easily split along the cleavage plane with a smooth - mirror surface.

The doping was performed by adding the corresponding weighted portion of lanthanum to the cell with the preliminarily synthesized $TlInS_2$ compound. The resulting La - doped ingot was yellow in color, showed good optical quality and its freshly cleaved surfaces were mirror like. The chemical composition of the crystals was determined by energy dispersive analysis using a scanning electron microscope. This analysis demonstrated that the doped $TlInS_2$ sample is enriched by the lanthanum impurity with a content of ~ 0.37 at. %.

Sample for the electrical measurements was cut from the single crystal ingot parallel to [010] axis. The active area and thickness of the sample were about 4.5 mm^2 and 2.5 mm respectively. Methyl alcohol solution was used as cleaner for crystal faces. High - purity silver paste was coated on two opposite faces of the sample as electrodes. A thin copper wire was attached to the electrodes by silver paste drop for the measuring circuit. The sample was placed inside a close - cycle helium optical cryostat equipped with a temperature stabilization system with an accuracy of ~ 0.05K. The temperature was measured and controlled by a Lake Shore - 340 model temperature controller. The temperature was measured by a DT - 470 silicon diode sensor. The experimental setup was fully computer controlled.

The ferroelectric hysteresis loops property of the $TlInS_2$: La capacitor was investigated by using computer controlled modified Sawyer - Tower circuit with voltage pulse of triangular wave type and with phase compensation of the linear part of the polarization and leakage. The polarization of the sample was derived from the charges of a capacitor connected in series with the sample. The electric field was applied to a sample by a high - voltage ***ac*** amplifier with the input sinusoidal signal with a frequency of 50 Hz from a signal generator. A computer program was used for displaying hysteresis loop traces from the monitor of the digital high resolution multi - channel oscilloscope at fixed temperatures.

A 100 W power halogen lamp with different filters was used for optical illumination of the sample in the P - E hysteresis loop measurements under illumination. With the purpose of achieving the greatest possible orientation of the polar La impurities the ***dc*** electric field about 20 kV/cm was applied to the sample in a direction parallel to the ***b*** – axis (the ***b*** – axis lies in the plane of layers). The sample was preliminarily cooled under dc electrical field from the room temperature down to ~ 13 K, and then the high voltage was removed from the sample and P - E hysteresis loop measurements at different temperatures were performed.

The measurements of ME were performed according to the following procedure. Firstly, the sample was cooled down to ~ 13K and then it was heated and annealed at T_{ann} ~ 210K within the INC - phase for ~ 5 hours. Then the sample was cooled again to ~ 80K and the P - E hysteresis loops at different temperatures were registered on the heating regime.

3. EXPERIMENTAL RESULTS

3.1. P - E hysteresis loops measurements in undoped $TlInS_2$

Fig.1 illustrates the typical bipolar ferroelectric P – E hysteresis loops for undoped $TlInS_2$ sample measured at 170K which is far below T_c. Hysteresis loops were plotted up to 40 kV/cm and with 50 Hz frequency. A clear reverse polarization hysteresis loops behavior was observed. The normal single hysteresis loop at $T \leq T_c$ provides additional evidence for the conclusion about the presence of the ferroelectric phase in $TlInS_2$ below the Curie temperature. The area inside the loop clearly increases with temperature decreasing indicating that the existence of the loop is due to the stable polarization.

As it is seen from the figure, the observed P – E hysteresis curve is slightly asymmetric both along the field and polarization axes. It has been observed that the negative coercive field is slightly higher than the positive one. There could be more than one contributor causing this asymmetry in the hysteresis behavior. We do not consider the reasons associated with different electrode materials of different work functions or different densities of interface states [27, 28], because of the same silver paste electrodes were deposited into opposite parallel cleavage planes for electrical measurements. The asymmetric shape of the hysteresis loop could also be attributed to the space charge layer near the one of the electrodes [27, 28], which decreases the electric field within the ferroelectrics. The width of space charge layer varies with the direction of polarization and therefore different near different electrodes. Hence the hysteresis loop is slightly asymmetric in shape [27, 28]. Additionally, a small discrepancy between the positive and negative values of remnant polarization (P_r) was observed.

The reason for choosing of the temperature 170 K as the reference point for study of ferroelectric switching in $TlInS_2$ is intentional. A change of shape in the hysteresis loops in the vicinity of phase transitions at T_i and T_c has been demonstrated in our previous work [3, 4, 6]. The P - E hysteresis loops of $TlInS_2$ modified from a single loops to a triple - like loops when the temperature increase above 170K up to T_c ~ 200K. The polarization - electric field hysteresis loops measurements were still possible above T_c at the temperatures up to ~ 204K. The triple - like P – E hysteresis loops have been gradually transformed to the double hysteresis loops in this temperature region. $TlInS_2$ possessed the normal single square – like hysteresis loops only at $T \leq$ 170K. The mechanism of such abnormal temperature transformation of the shape of ferroelectric hysteresis loops near the PT – points in $TlInS_2$ was discussed in [3, 4, 6].

The origin of the asymmetric hysteresis behavior in P – E plots of $TlInS_2$ is still not clear. However, it is known that asymmetric character of the hysteresis loops in ferroic materials originates from the internal fields [29]. It is also known that $TlInS_2$ is p - type semiconductor in which the acceptor impurities create deep - trapped levels with high relaxation time constants

[15 - 21]. The space charges trapped in these deep – levels generate the so-called built-in polarization, which is almost not sensitive to ferroelectric phase transition and ferroelectric (switchable) polarization that becomes spontaneous below the phase transition temperature T_c.

On the other hand, the second origin of the asymmetric $P – E$ hysteresis loops is an asymmetric space - charge distributions in metal - $TlInS_2$ interfaces. The ferroelectric hysteresis loop is also affected by the presence of these space charge regions so that $P – E$ hysteresis loops may be asymmetrically changed as in the case of built - in polarization from charged deep level traps.

The space charge effect on the ferroelectric hysteresis loops can be understood by the presence of a displacement current (I_d). When an external voltage in the form of triangular wave type is applied to the ferroelectric the I_d dynamics is given as [30, 31]:

$$I_d = \frac{d(CV)}{dt} = V(t)\frac{dC(t)}{dt} + C(t)\frac{dV(t)}{dt}, \qquad (1)$$

where C – is the capacitance of the metal – ferroelectric - semiconductor crystal interface(s) and $V(t)$– is added to the contact external voltage. For semiconductor - ferroelectric crystals the contribution of capacitance variation $V(dC/dt)$ on the displacement current is much stronger than that due to the voltage variation$C(dV/dt)$. Therefore, $I_d \approx V(dC/dt)$. The capacitance can vary due to the formation of space charges at the metal - ferroelectric - semiconductor interface(s). Moreover, the space – charge densities at metal – ferroelectric - semiconductor interface(s) is dependent of the external voltage amplitude.

3.2. Native deep defect levels in undoped $TlInS_2$ and $TlInS_2$: La

Sub – band gap PICTS analysis of the deep trap levels in undoped $TlInS_2$ revealed the existence of five major traps. In the PICTS spectra a deep defect level labeled as TE2 at $E_t = 0.16$ eV was detected. TE2 is activated in the temperature region $\Delta T = 93 – 110$K and has the capture cross – section $\sigma = 6.9 \times 10^{-15} cm^2$ [15-21]. A similar trap was found with PICTS measurements of $TlInS_2$: La ($E_t = 0.17\ eV,\ \Delta T = 96 - 108\ K,\ \sigma = 2.2 \times 10^{-14} cm^2$) [15 - 21]. It is worth noting that the PICTS method does not determine the trap sign i.e., it is a majority or minority carrier trap. Therefore, it is hard to state if the measured activation energy E_t has to be calculated from the valence or the conduction band. To properly identify the level, one has to relate the PICTS results to other trap characterization methods. This is why we do not specify either the native deep acceptors or donors which are related to deep level defects detected using the PICTS – method in $TlInS_2$.

The other deep level defect determined by PICTS experiments in undoped $TlInS_2$ (labeled as BT23) is located at $E_t = 0.25\ eV$. BT23 and activated in the temperature region $\Delta T = 115 – 135$K having the capture cross – section of $\sigma = 2.9 \times 10^{-16} cm^2$ [15 - 21]. A similar trap was also found with PICTS measurements of $TlInS_2$:La($E_t = 0.20\ eV,\ \Delta T = 113 - 135\ K,\ \sigma = 5.8 \times 10^{-13} cm^2$) [15 - 21].

The B5 deep level defect at $E_t = 0.3$ eV is the major trap which was detected in PICTS studies of undoped $TlInS_2$. The temperature of activation and the capture cross – section of this native deep level defects are $\Delta T = 190 - 240K$and $\sigma = 1.8 \times 10^{-16} cm^2$ respectively. It is worth noting that the active state of B5 - deep trap coincides with the temperature region of PT in $TlInS_2$ ternary compound [15 - 21]. A similar trap has, in fact, been found in PICTS measurements of $TlInS_2$: La ($\Delta T = 192 - 234\ K$, with the same activation energy and carrier capture – cross section as in undoped $TlInS_2$). The deep level centers marked as B7 and D_0 in undoped $TlInS_2$ [15 - 21] and TE54 in $TlInS_2$: La are responsible for the charge emission at the temperature ranges of $\Delta T = 240 - 300\ K, 316 - 330\ K$ and $268 - 307\ K$ respectively that is much above the Curie temperature. We focused our attention on the study of the native deep level centers in undoped $TlInS_2$ and $TlInS_2$: La which are ionized in the vicinity of PT and thus dramatically affected the shape of the ferroelectric hysteresis loops at the temperatures lower thanT_c. Therefore, the native deep level centers B7 and D_0 in undoped $TlInS_2$ and TE54 in $TlInS_2$: La crystals are not considered here.

PICTS measurements on $TlInS_2$: La sample showed the presence of so - called BTE43 deep level traps at $E_t = 0.29\ eV$ ($\sigma = 2.2 \times 10^{-14} cm^2$) [15 - 21]. This defect has a thermal emission interval below the Curie temperature ($\Delta T = 156 - 176\ K$). This defect is registered in $TlInS_2$: La only. It must be mentioned that, the experimental data presented in [15 - 21] do not clearly allow any conclusion about the origin of deep level center in $TlInS_2$: La observed by PICTS – method. We believe that BTE43 deep level defect is related to La – dopant.

3.3 The *P - E* hysteresis loops in electro – thermally poled $TlInS_2$

In order to investigate the contribution of each charged native deep level defect to polarization properties of $TlInS_2$ crystal we studied changes of the ferroelectric $P – E$ hysteresis loops shape after electro - thermal poling of crystal. During the electro – thermal poling process, a static external electric field of intensity ~ 20 kV/cm was applied on the samples at the temperature range where the corresponding deep level defect is thermally activated.

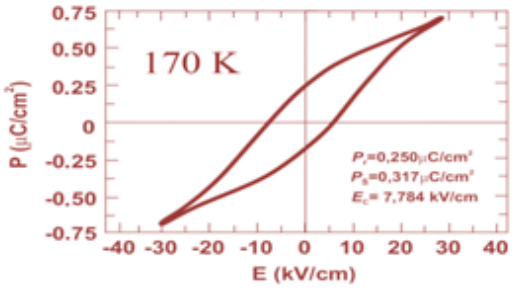

Fig. 1 - Polarization - electric field (*P - E*) hysteresis loop of unpoled $TlInS_2$ measured at a frequency of 50 Hz and at 170K. The inset shows the values of remanent polarization (P_r), saturated polarization (P_s) and a coercive field (E_c).

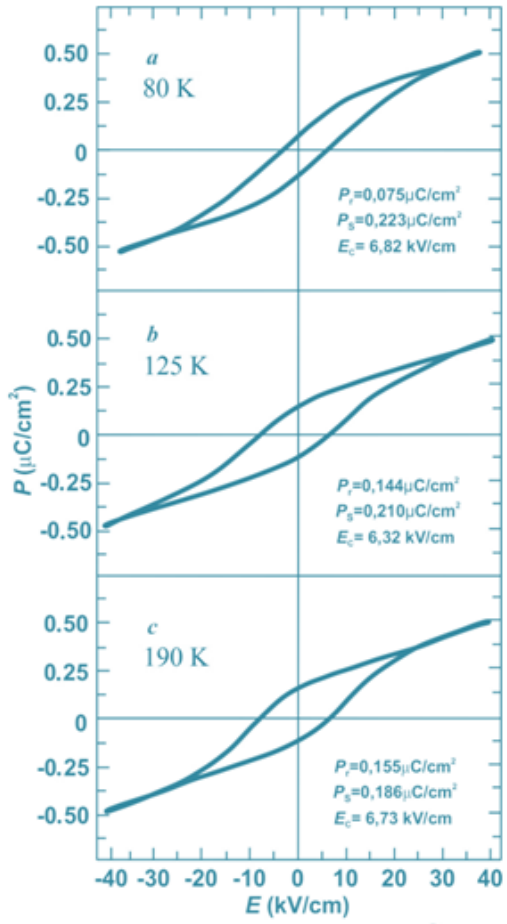

Fig. 2. Polarization versus electric field hysteresis loops of unpoled $TlInS_2$ measured at different temperatures: a) 80, b) 125, and c) 170 K after crystal polling procedure under external electric field of intensity ~20 kV/cm applied to the samples at the temperature range ~190 – 240 K, where the B5 deep level defects are thermally activated. The inset shows the values of remanent polarization (P_r), saturated polarization (P_s) and a coercive field (E_c).

A poling voltage of 1 kV is applied for a period of typically 20 ~ 30 minutes. After the poling process the applied voltage was removed. Finally, the sample is cooled down to 80K. Thus, at low temperatures the charged defects and the defect dipoles remain in their original orientation during the P - E loop measurement, and may induce the ferroelectric loops shape changing. In order to investigate the effect of poling voltage on the P – E hysteresis loops, electro – thermally poled $TlInS_2$ sample was studied at 80, 125, and 170K.

The hysteresis loops of the $TlInS_2$ with activated so – called B5 deep level defects are indicated in Fig. 2. It is seen that two P - E loops shown in Fig. 1 and 2 (a) are obviously different. The sample with charged B5 deep level defects exhibits well - defined normal single hysteresis loops with data of remnant polarization (the remnant polarization (P_r) is a non - zero polarization observed at zero electric field), saturated polarization (the saturate polarization (P_s) is equal to the polarization in the linear fit of P versus E extrapolated at zero electric field) and a coercive field (the coercive field (E_c) is a non - zero electric field observed at zero polarization) which is relatively smaller than that in Fig. 1. Accordingly, the P - E loops of $TlInS_2$ with activated B5 defects becomes more saturated on decreasing the temperature, as shown in Fig. 2 (b and c).

It is well known that hysteresis behavior of the polarization mainly originates from the ferroelectric domain switching under an external electric field. Usually, the switching process of domain in ferroelectrics suffers a certain resistance or viscous drag force [1, 32]. The resistance of viscous drag force generally increases with increasing mobile free charges, vacancies and other ion defects. If these charged defects cannot follow the applied electric field the polarization decreases [1, 32].

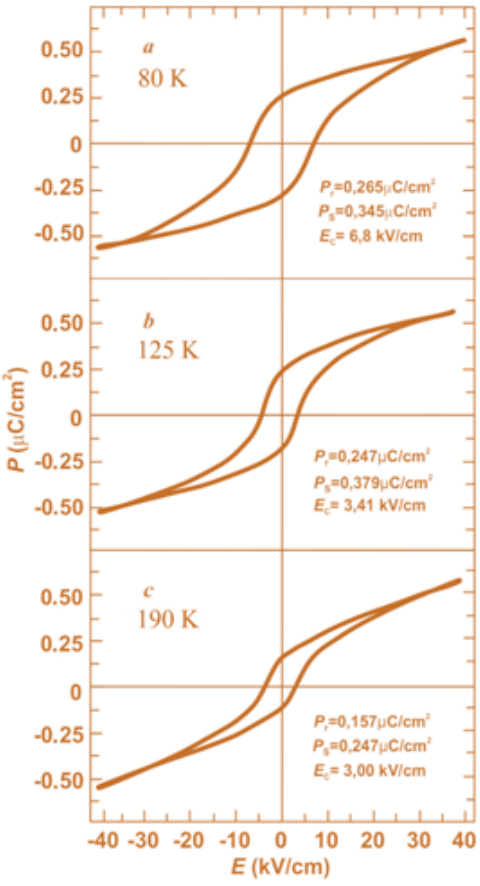

Fig. 3. Same as Fig. 2, but the sample was polled in the temperature region ~ 120 – 135 K, where the BT23 deep level defects are thermally activated. The inset shows the values of remanent polarization (P_r), saturated polarization (P_s) and a coercive field (E_c).

Figure 3 shows the polarization versus applied field response of the undoped $TlInS_2$ sample with activated BT23 native deep defects measured at 80, 125 and 170K. $TlInS_2$ exhibits rather well developed, symmetric and saturated hysteresis loop with sharp ends. Additionally, the temperature behavior of the hysteresis loops revealed that both the remanent polarization and coercive field decrease on increasing the temperature. It can be supposed that the internal electric field originated from charged BT23 native deep defects could be the reason of domain pinning which brings to reduce of P_r. The increasing domain pinning of defects implied by the decreasing E_c. The diminishing fraction of domains which

can be switched as distinct from frozen ones located in the regions where an internal electric field originated from ionized BT23 native deep level centers are imprinted might be a dominant factor of total ferroelectric polarization reduction.

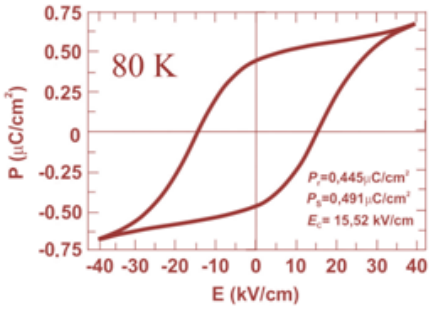

Fig. 4. $P - E$ hysteresis loop of unpoled $TlInS_2$ measured at 80 K after crystal polling under external electric field of intensity ~ 20 kV/cm applied to the samples at the temperature region ~ 95 - 110 K, where the TE2 deep level defects are thermally activated. The inset shows the values of remanent polarization (P_r), saturated polarization (P_s) and a coercive field (E_c).

Fig. 4 shows a remarkable ferroelectric P - E hysteresis loop in terms of its shape and area evolution measured at 80K after electro – thermally poling of undoped $TlInS_2$ sample inside the temperature region where TE2 deep level traps are activated. The hysteresis loops are saturated, and exhibit clear nonlinear character without loss contribution. The shape of P - E curve in the terms of geometric configuration is Single Square – like with a rectangular factor of ~ 0.15. The value of saturation polarization (P_s) and remanent polarization are provided in Fig. 4. It is noted that the shape of $P - E$ hysteresis loops shown in Fig. 4 is typical for ferroelectric materials where no apparent pinning phenomenon exists, indicating that crystal structure defects are less.

It is well known that the ferroelectric phase is essentially the cooperative phenomena, which is stabilized by the long range coulomb interaction of electric dipole moments that appears spontaneously in each cell. Hence, there are several factors which are responsible for energy loss in dielectric materials. Crystal defects, inhomogeneity's, domain boundaries, and pores are the internal sources for energy losses. In defective ferroelectric crystal with charged deep level centers, more and more ferroelectric domains are constrained by the applied stress and cannot be re - oriented by the electric field so as to participate in the polarization reversal. Furthermore, it is noted that electric field cloud surrounding each ionized deep level defects could be reduce the sample volume (due to the growth of the frozen domains fraction) involved into polarization reversal processes.

The energy density of the dielectric materials can be calculated using the integral $\oint EdD$, where E is the applied electric field on the materials, $D(T) = \varepsilon_0 E + P(T)$ is the temperature evolution of electric displacement and $P(T)$ is the total polarization that is a sum of induced and spontaneous polarization of material. In ferroelectric materials, $D(T)$ is approximately equal to $P(T)$. Generally, the spontaneous polarization gives the main contribution in temperature dependence of $P(T)$. Geometrically, the integral the integral $\oint EdD$ means the area enclosed by P - E curve [33 - 36].

On the other hand, the temperature dependence of spontaneous polarization (P_{spon}) of improper ferroelectrics below of the phase transition temperature T_c has the form [33 - 36]:

$$P_{spon} = \Upsilon \cdot (T_c - T)^2, \qquad (2)$$

where Υ is constant composed from the Landau thermodynamic potential coefficients. It is obviously, that the area of ferroelectric P - E hysteresis loop should increase with a decrease in temperature.

Physically, the integral $\oint EdP$ indicates the polarization dissipation energy subjected to one full cycle of electric field application, and the loop area is therefore directly related to the crystal volume involved in the switching process during the application of the electric field. In other words, the area enclosed by the P - E curve and polarization axis represents the ratio of non - polar phase regions contained in the volume of sample to polarized ones.

To understand at least qualitatively the experimental results related to the contribution of each of charged native deep level defects in polarized properties of $TlInS_2$ ferroelectric - semiconductor, one needs to consider the following statements. Electro - active materials, which are able to retain electric polarization over a long period of time and create an internal static electric field, are known as electrets [37 - 40]. It is well known that electret behavior of semiconductor materials arises from both the dipole orientation and the charge storage. The internal electric field in semiconductor materials submitted to an external electric field may originate from hetero – and homo - charges [37- 40]. An internal electric field is created by space charges accumulated in the trap levels in the regions directly adjacent to the electrodes (homo - charge) as well as in the bulk region of the crystal (hetero - charge) [37 - 40]. The internal electric field created by homo - charges has the same direction as the field applied to the sample. The field created by hetero - charges formed in the bulk region of crystal and originated from ionized native deep level defects has the direction opposite of the direction of applied field.

When the native deep level defects B7, B5 and BT23 are activated by previously electrothermal poling of crystal, the internal electric field inside the crystal from charged deep level centers has the direction opposite to the direction of an external poling field [14, 16 – 20, 22 – 28, and 37 - 41]. This imprinted internal field tends to keep the ferroelectric domains aligned away from the direction of the applied electric field preventing reorientation of the domains along the external applied field direction resulting in a lower value of saturated polarization (Figs. 2 and 3). When the applied (Sawyer – Tower) electric field is reduced to zero and then changes the direction, the domain unable to rotate back away due to the frozen internal electric field. This leads to a reduction of remnant polarization in comparison with ones measured on $TlInS_2$ crystals with non - activated

deep level defects (Fig. 1). The decrease of the integral $\oint EdP$ area in Fig. 4 indicates that more and more ferroelectric domains are involved in polarization switching process and can be reoriented by the applied electric field. Thus, in undoped $TlInS_2$ sample with non – activated deep level defects or in the same sample with activated B7, B5 and BT23 deep level centers not the whole $TlInS_2$ ferroelectric crystal volume is involved in the polarization reversal process.

3.4 The *P* - *E* hysteresis loops of $TlInS_2$: La poled under different external fields

In order to gain further insight into the role of La doping, hysteresis loops of $TlInS_2$ with ~ 0.3 mol % La were measured at several temperatures on heating. Typical for $TlInS_2$: La sample *P* - *E* hysteresis loops measured at 80 K have been plotted in Fig. 5 (a). It can be observed that these loops do not saturate even under an applied field of 40 kV/cm. With temperature increase the shape of hysteresis loops shrinks from sharp - tip rhombic to very slim. The dielectric loop pattern in $TlInS_2$: La was observed at temperature below ~ 150 K only.

It is known that La doping induces the formation a lattice distortion in crystalline structure $TlInS_2$. This can be explained by saying that the ion radius of La^{3+} 0.187 nm) cation is larger than ones for Tl^{+} (0.149 nm) and In^{3+} (0.092 nm). The internal stress is due to by La additions can be considered as polar micro – domains. Obviously, the ferroelectric macro - domain state in $TlInS_2$ became more and more unstable at the temperature range where BTE43 deep level traps related to La dopant are active ($\Delta T = 156 – 176K$).

A double *P* - *E* hysteresis loops is observed in the same $TlInS_2$: La sample at T ≤ 150K after thermally poling of sample by an external electric field in the temperature region where BTE43 deep level traps are activated and under the illumination, as shown in fig.5(b). To investigate the origin of the double *P* - *E* loops in $TlInS_2$: La possible influences of light with different wavelength that can affect the *P* - *E* hysteresis loops of $TlInS_2$: La sample were checked. The function of the background illumination is to excite electrons from the valence band of $TlInS_2$: La into deep level traps, thus keeping the traps full with electrons, and leave holes in the valence band. To do this, the xenon lamp with set of different optical filters was used. Various excitation wavelengths of more than ~ 540 nm (the wavelength corresponding to the forbidden gap of $TlInS_2$) can be used as background illumination. According to the results of our experiment, ~ 700 nm is the best wavelength for the background. Stable and pronounced double *P* - *E* hysteresis loops under the background illumination of ~ 700 nm with red filter were observed. Despite extensive efforts, the physical origin of the double *P* - *E* hysteresis loops in $TlInS_2$ layered semiconductor with La additions remain were unclear. We can only assume that BTE43 deep level traps related to La dopant can be electrically activated on thermal poling of $TlInS_2$: La sample by an external electric field and under the illumination. The ionized BTE43 defects can lead to the release of free carriers either in the conduction band or in the valence band and transform to defect dipole. These defect dipoles can pin the ferroelectric domains irreversibly and induce the double *P* - *E* hysteresis loops.

Rather unexpected change of the shape of *P* - *E* hysteresis loops of the same $TlInS_2$: La sample was observed after annealing of the crystal for 5 h within the INC – phase at 210 K. A triple – like hysteresis loop at low temperatures as manifestation of a memory effect was detected in $TlInS_2$: La crystal. This triple hysteresis loops consists of three loops in which two of them are the inversions of each other about the origin and one is central loop, as seen in Fig. 5 (c). Note that, the presence of the central loop means the appearance of a new component in the crystal polarization at low temperatures [42, 43]. One may deduce that the triple *P* - *E* hysteresis loop behavior is related to the interaction of BTE43 defects with DDW. It should be noted that neither double – like nor triple hysteresis loops were observed in undoped $TlInS_2$ under similar experimental conditions.

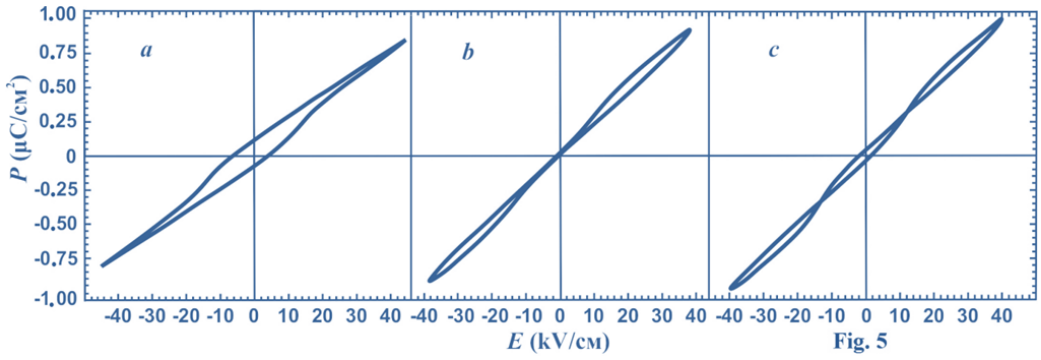

Fig. 5. Multipolar *P* – *E* hysteresis loops of La doped $TlInS_2$ sample measured at 80 K; a) under normal conditions; b) after sample poling by an external electric field and after the illumination of crystal by visible light of ~ 700 nm wavelength in the temperature region ~ 155 – 175 K, where BTE43 deep level traps are thermally activated; c) after crystal annealing for 5 h inside the INC – phase.

In summary, five types of native deep trap levels in undoped and La – doped $TlInS_2$ ferroelectric semiconductor have been identified in our previous work [14 - 21]. These traps act as charge storage centers and can be served as origin of the internal electric fields inside the material. It was found, that BTE43 deep level defect is related to La – dopant because of its absence in undoped $TlInS_2$. In this study, the effect of each activated deep level defect on the polarization properties of $TlInS_2$ and $TlInS_2$:La was investigated by using *P* - *E* ferroelectric

hysteresis loop measurements. Deep level defects in both samples were activated at different temperatures by an external electric field, light illumination and long-time thermal annealing procedure inside the INC - phase in the memory effect regime. Special attention is given to BTE43 deep level defect. As a result, multiple *P* - *E* hysteresis loops in $TlInS_2$:La were found depending on the activation way of this type of defect. Finally, observations presented in this paper are consistent with earlier investigations of the effect of native deep level defects in $TlInS_2$ and $TlInS_2$:La on their electric, ultrasonic, pyroelectric and thermally depolarization properties recently published in literature [14 - 21].

5. DISCUSSION

Firstly, we note that the analogy between domain walls movements in ferroelectric crystals and damped mechanical oscillator model gives good results for the study of switching of crystal polarization under the electric field. We can obtain a perfect fit between measured ferroelectric hysteresis loop curves and the simplest model of friction - induced vibrations consisting of a spring - mass - damper system. It has been demonstrated here that the universal nonlinear oscillator behavior may be identified by studying of *P* - *E* hysteresis loops phenomena. The understanding and modelling of *P* - *E* hysteresis loops in undoped $TlInS_2$ and $TlInS_2$: La under external excitations will allow to establish the mechanical analog of deep level defects and physically the mechanical analogies of ME.

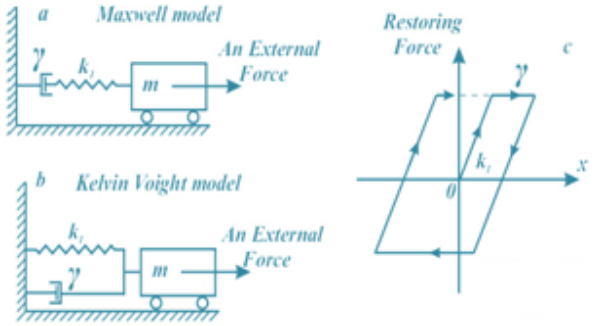

Fig. 6. Schematic diagram of Maxwell (a) and Kelvin - Voigt (b) oscillatory model; c) A typical hysteresis cycle of restoring force vs. displacement for Maxwell and Kelvin - Voigt models under a sinusoidal external excitation.

We consider an oscillator system with a single degree of freedom consisting of a mass, a Hookean elastic spring, and a Newtonian damper (or dashpot). The mass is moving on a smooth surface without friction. The Maxwell oscillatory model called a model when the elastic spring and the dashpot element are connected in series as it is shown in Fig. 6 (a). The Kelvin – Voigt model is shown in Fig. 6 (b) where the spring element and dashpot are connected in parallel [44 - 50]. The constitutive equation of motion for such mechanical systems is described by the ordinary differential equation:

$$m\frac{d^2x}{dt^2}+\gamma\frac{dx}{dt}+k_1x=f_0\cos(\omega t), \qquad (3)$$

where x is the displacement, m is the oscillator mass, γ is the dissipation or damping coefficient, k_1 is the linear spring constant, $f_0\,cos(\omega t)$ denotes a periodic force applied to the system and f_0 is the force amplitude. To compare with our data, $f_0\cos(\omega t)=|e|E(\omega_{ST}t)$, where $|e|$ is the electron charge and $E(\omega_{ST}t)$ is the electric field pulse in a triangular wave type with the Sawyer - Tower circuit frequency $\omega_{ST}=50$ Hz.

We orient the system along the x - axis, and let $x=x(t)$ denote the horizontal displacement of the attached mass m from the static equilibrium position $x=0$ of the spring. For the case of simplicity we assume that the periodic external force has the form of a sine – wave ($eE_{max}\sin\omega_{ST}t$) or even a rectangular wave with the frequency ω_{ST}. Also one assumes that the material is completely rigid.

The differential equation (1) describes the behavior of the linear oscillator with eigenfrequency $\omega_0=\sqrt{k_1/m}$. Typical restoring force (normalized by the mass of the oscillator) vs. displacement relationship for Maxwell / Kelvin – Voigt model for illustration purposes is depicted in Fig. 6. The idea of this model is as follows: When the displacement increases or decreases continuously, the gain between the force and the displacement changes piecewise linearly.

Let us suppose that the motion is started from the rest by moving the mass m to the right under an external force. An external force in the beginning will deform an elastic spring.

The mechanical energy stored in the elongated elastic spring (for smaller elongation in magnitude) will take to overcome the friction force in the damper. The extra positive displacement will be in oscillatory system even when the external force changes direction.

The mechanical restoring force - displacement hysteresis loops will take place in Maxwell or Kelvin – Voigt oscillatory systems. Obviously that the area overlapping by hysteresis loop curve will depend on its internal parameters; the damping coefficient (γ) and elastic spring constant (k_1).

From visual inspection of the hysteresis loops shown in Figs. 1 – 3 and 6 one can assume that thermally – electro activation of B7, B5 and BT23 deep level defects in $TlInS_2$ is equivalent to changing of the mechanical parameters γ and k_1 in Maxwell or Kelvin – Voigt oscillatory models.

The double restoring force – displacement hysteresis loops is observed for nonlinear oscillatory system when a nonlinear spring (Voigt element) is added in series with damper element, as it is shown in Fig. 7.

The nonlinearities of the spring are taken into account by adding the term of k_3x^3 – a cubic restoring force in the equations of motion (3). Here k_3 is the cubic stiffness parameter. For $k_3>0$ the spring hardens with increasing displacement (spring hardening), for $k_3<0$ the spring softens with increasing displacement (spring softening).

Figure 7 (b) shows a schematic representation of the double restoring force – displacement hysteresis loops.

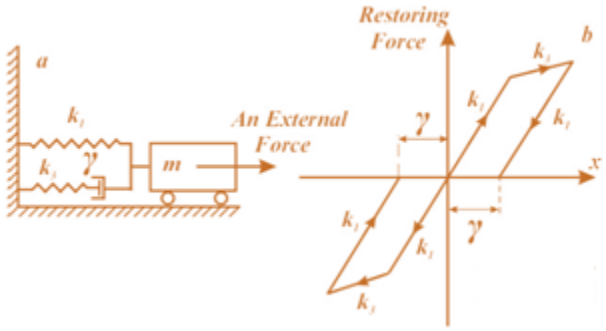

Fig. 7. a) Schematic set - up for single degree of freedom non – linear damper oscillatory model. b) Restoring force versus displacement double hysteresis loop for non - linear damper oscillatory model.

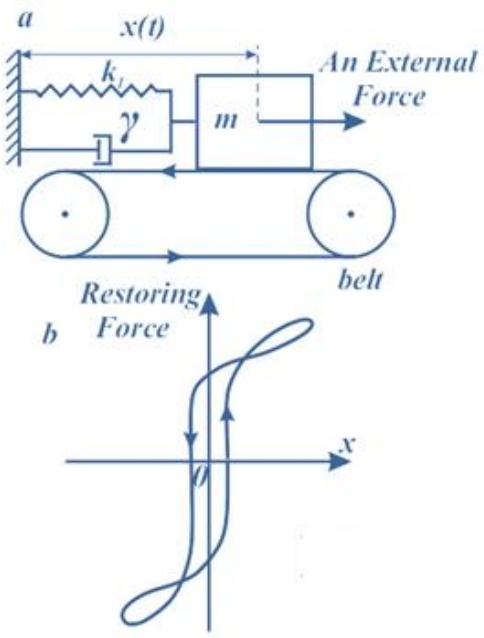

Fig. 8. a) A schematic plot of the damped harmonic oscillator on a moving belt as a model of harmonic oscillator damped by Coulomb friction; b) Triple hysteresis loop characteristics of the restoring force as a function of the displacement for such model.

Finally, let's consider a single degree of freedom spring - mass - damper oscillator model in which the mass resting on a moving belt. The physical system is shown in Fig. 8. The equation governing the motion of the oscillator shown in Fig. 8 is given by:

$$m\frac{d^2x}{dt^2} + \gamma\frac{dx}{dt} + k_1x + F_{friction} = f_0\cos(\omega t), \quad (4)$$

We added the friction to the system, since the mass – spring - damper is contacted with moved belt that causes friction. We describe it with the Coulomb law of dry friction, in which the friction resistance force is $F_{friction} = -\mu mg \cdot sgn(v_r)$. Here, μ is the coefficient of friction and g is the gravitational acceleration; $v_r = v_{belt} - \dot{x}$ is the relative velocity. The friction resistance force is opposite to the direction of motion, represented by the function $sig(v)$, which is given by [44 - 51]:

$$sgn(v) = \begin{cases} 1, & if\ v > 0 \\ 0, & if\ v = 0 \\ -1, & if\ v < 0 \end{cases}$$

In (4) for simplicity we assume that the periodical potential friction is sinusoidal and k_3 is zero.

The evolution of the oscillator state is described by the differential equation (4). This state can be in different acceleration and deceleration phases depending on the sign of the relative velocity giving different contributions to the friction forces. Hence, the restoring force – displacement curve follows different paths for acceleration and deceleration phases resulting in triple – type hysteresis loops form which is due to non - reversible friction.

The relation between the displacement of the oscillator and the restoring force is depicted schematically in Fig. 8 (b). It should be noted that a spring - mass - damper oscillator model with the Coulomb dry - friction have be used for modelling of triple – type I – V hysteresis loops in the charge – density wave solids [52, 53].

By visual inspection of the shape of hysteresis loops shown in Fig. 4 and in Figs. 7 and 8 one can conclude that the mechanical prototype of charged BTE43 deep level defects is a nonlinear spring attached in series with damper. Activation of BTE43 deep level defects by the external electric field or by photo – excitation causes the energy dissipation in ferroelectric material due to the spatially inhomogeneous polarization initiated by BTE43 deep level defects, which role is similar to that of the nonlinear spring in an oscillator model.

Mobile defects and their spatial long range ordering (DDW) are often invoked as the microscopic explanation of some experimental observations inside the intermediate INC - phase of ferroelectric crystals such as thermal hysteresis effects and specific ME. In $TlInS_2$ as well as $TlGaSe_2$ it has been hypothesized that DDW - modulation interacts with the incommensurate modulation resulting in many intriguing properties at low temperatures which are still not explained [5, 8, 14 - 21]. DDW is a periodic distortion of the crystal lattice due to by periodic displacements of the atoms from their normal positions. Lattices deformed in this way initiate the micromechanical inelastic stress and strain fields inside the crystal [52, 54, 55]. The mechanical analogy of DDW is internal friction which characterizes energy dissipations at mechanical loading. Thus spring - mass - damper oscillator moving in the presence of the Coulomb friction is the mechanical prototype of the ME in $TlInS_2$: La. Charged BTE43 deep level defects interacting with domain wells in a "electrically viscous" surrounding is the origin of triple – type P – E hysteresis loops in $TlInS_2$: La.

4. CONCLUSIONS

Thus, the experimental investigation of the effect of deep level defects on ferroelectric hysteretic loops in undoped $TlInS_2$ and $TlInS_2$:La has been performed. The P – E hysteresis loops were studied as a function of temperature inside the ferroelectric phase at various external electric field intensities. It has been revealed that

in undoped $TlInS_2$ sample the activated B7, B5, BT23 and TE2 deep level centers greatly affect the geometrical shape (saturated and unsaturated loops) and parameters (coercive field, remnant and saturated polarization) of dielectric hysteresis loops.

The effect of deep level defects on *P* - *E* hysteretic loops in $TlInS_2$: La sample is fully different from undoped $TlInS_2$. The double – type hysteresis loops have been detected in $TlInS_2$: La at all temperatures below ~ 190K after activation of BTE43 deep level defects by external electric field poling procedure. Furthermore, the double – type hysteresis loops were revealed in $TlInS_2$: La under activation of BTE43 deep level centers by background illumination. Unexpectedly, triple – type dielectric hysteresis loops were observed in $TlInS_2$:La at $T < 190$K after annealing of the sample during 5 hours within the INC – phase. It has been assumed that BTE43 deep level traps are corresponded to La – dopant. Different type spring - mass - damper oscillator models are involved in order to qualitatively understand the mechanical analogues of observed phenomena. The dramatic increase in the internal friction in $TlInS_2$ as a result of ME is the main result of the present investigation.

ACKNOWLEDGEMENTS

MS and FM acknowledge support from The Scientific & Technological Research Council of Turkey (TÜBİTAK) through the bilateral program RFBR (14-02-91374 CT_a) – TUBITAK (No. 213M524).

[1] *M.E. Lines, A.M. Glass.* Principles and Applications of Ferroelectrics and Related Materials (Oxford Clarendon, 1977).

[2] *B.A. Strukov, A.P. Levanyuk.* Ferroelectric Phenomena in Crystals (Springer, 1998).

[3] *R .A. Suleimanov, M. Yu. Seidov, F.M. Salaev and F. A. Mikailov*. Phys. Solid State 35, 177 (1993).

[4] *K.R. Allakhverdiev, N.D. Akhmed-zade, T.G. Mamedov, T.S. Mamedov, M.Yu. Seidov*. Low Temperature Physics 26, 56 (2000).

[5] *M-H. Yu. Seyidov, R. A. Suleymanov, S. S. Babayev, T.G. Mammadov, A.I. Nadjafov, and G.M. Sharifov.* Phys. Solid State 51, 264 (2009).

[6] *F.M. Salaev, K. R. Allakhverdiev and F. A. Mikailov*. Ferroelectrics 131, 163 (1992).

[7] *F.A. Mikailov, E. Başaran, T.G. Mammadov, M.Yu. Seyidov, E. Şentürk.* Physica B, 334 13 (2003).

[8] *S.S. Babaev, E. Basaran, T.G. Mammadov, F. A. Mikailov, F. M. Salehli, M-H. Yu. Seyidov, R.A. Suleymanov.* J. Phys.: Condens. Matter, 17 1985 (2005).

[9] *H. Hahn, B. Wellman.* Naturwissenschaften B. 4, 42 (1967).

[10] *T.J. Isaacs, T.D. Feichtner.* J. Solid State Chem. 14, 260 (1975).

[11] *S. Ozdemir, M. Bucurgat.* Current Applied Physics 13, 1948 (2013).

[12] *M.M. El - Nahass, M.M. Sallam, A. H. S. Abd Al – Wahab.* Current Applied Physics 9, 311 (2009).

[13] *O.V. Korolik, S.A.D. Kaabi, K. Gulbinas, N.V. Mazanik, N.A. Drozdov, V. Grivickas*. J. Luminescence, 187, 507 (2017).

[14] *M-H. Yu. Seyidov, R. A. Suleymanov, F. Salehli.* J. Appl. Phys. 108 024111 (2010).

[15] *M-H. Yu. Seyidov, R. A. Suleymanov, A. P. Odrinsky, A. I. Nadjafov, T. G. Mammadov, E. G. Samadli.* Jap. J. Appl. Phys. 50, 05FC08 (2011).

[16] *A. P. Odrinsky, T. G. Mammadov, MirHasan Yu. Seyidov, V. B. Aliyeva*. Physics of the Solid State 56 1605 (2014).

[17] *MirHasan Yu. Seyidov, A.P. Odrinsy, RA. Suleymanov, E. Acar, T. G. Mammadov, V. B. Aliyeva.* Physics of the Solid State 56, 2028 (2014).

[18] *MirHasan Yu. Seyidov, R. A. Suleymanov, E. Acar, A. P. Odrinsky, T. G. Mammadov, A. I. Nadjafov, V. B. Aliyeva.* Low Temperature Physics 40, 830 (2014).

[19] *MirHasan Yu. Seyidov, R. A. Suleymanov, F. A. Mikailzade, E. Orhan Kargın, A. P. Odrinsky*. Japan Appl. Phys. 117, 224104 (2015).

[20] *MirHasan Yu. Seyidov, R. A. Suleymanov, C. Kırbaş, A.P. Odrinsky*. Physica B. Cond. Mat. 497, 86 (2016).

[21] *MirHasan Yu .Seyidov, R. A. Suleymanov, F. Salehli, S. S. Babayev, A. I. Nadjafov, T. G. Mammadov, G. M. Sharifov.* Physics of the Solid State 51, 568 (2009).

[22] *J.P. Jamet, and P. Lederer.* J. Phys. (Paris) Lett. 44, L-257(1983).

[23] *J.P. Jamet, and P. Lederer.* Ferroelectric Lett. 1, 139 (1984).

[24] *P. Lederer, G. Montambaux and J. P. Jamet.* J.Phys.(Paris) Lett. 48, L-627(1984).

[25] *P. Lederer, G. Montambaux and J. P. Jamet.* Mol. Cryst. Liq. Cryst. 121, 99 (1985).

[26] *P. Lederer, J.P. Jamet, and G. Montambaux.* Ferroelectrics 66, 25 (1986).

[27] *J. Lee, C. H. Choi, B. H. Park, T. W. Noah and J. K. Lee.* Appl. Phys. Lett. 72, 3380 (1998).

[28] *K. Abe, S. Komatsu, N. Yanase, K. Sano and T. Kawakubo.* Japan. J. Appl. Phys. 36, 5846 (1997).

[29] *M. Alguero, J.M. Gregg, and L. Mitoseriu.* Nanoscale Ferroelectrics and Multiferroics, vol.1 (John Wiley & Sons Ltd, 2016)

[30] *A.G. Milnes.* Deep Impurities in Semiconductors (Jonh Wiley&Sons, New York, London, Sydney, Toronto, 1973)

[31] *M.A. Lampert and P. Mark.* Current Injection in Solids (Academic Press, New York, London, 1970)

[32] *A.S. Sidorkin.* Domain Structure in Ferroelectrics and Related Materials (Cambridge International Science Publishing, 2006)

[33] *K. Uchino.* Ferroelectric Devices (CRC Press, Taylor & Francis Group, 2010)

[34] *Y. Xu.* Ferroelectric Materials and their Applications (Elsevier Science Publishers B.V., 1991)

[35] *H.D. Megaw.* Ferroelectricity in Crystals (London: Methuen, 1957)

[36] *S.B. Lang, and H.L.W. Chan.* Frontiers of Ferroelectricity (Springer Science+Business Media LLC, 2007)
[37] *G.M. Sessler.* Journal of Electrostatics 51 – 52 (2001) 137 – 145.
[38] *G.M. Sessler* (ed.) Electrets. Topics in Applied Physics v. 33 (Springer, 1987)
[39] *V. M. Fridkin.* Ferroelectrics - Semiconductors (New York Consultants Bureau, 1980)
[40] *V.M. Fridkin.* Photoferroelectrics (Berlin Springer, 1979)
[41] *MirHasan Yu. Seyidov, R. A. Suleymanov, R. Khamoev.* Phys. Solid State 48 (2006) 1346 – 1350.
[42] *M.E. Lines, A.M. Glass.* Principles and Applications of Ferroelectrics and Related Materials (Oxford Clarendon, 1977)
[43] *B.A. Strukov, A.P. Levanyuk.* Ferroelectric Phenomena in Crystals (Springer, 1998)
[44] *F.C. Moon, Chaotic Vibrations.* An Introduction for Applied Scientists and Engineers (John Wiley & Sons, Inc., 2004)
[45] *L. Meirovitch.* Fundamentals of Vibrations (McGraw-Hill Book Co. Singapore, 2001) and Elements of Vibration Analysis (McGraw-Hill, Boston, Massachusetts 1986).
[46] *G.T. Houlsby and A.M. Puzrin.* Principles of Hyperplasticity. An Approach to Plasticity Theory Based on Thermodynamic Principles (Springer-Verlag London Limited 2006).
[47] *A.H. Nayfeh, and D.T. Mook.* Nonlinear Oscillations (Wiley Classics Library Edition Published 1995)
[48] *S.H.H. Kachapi, and D.D. Ganji.* Dynamics and Vibrations. Progress in Nonlinear Analysis (Springer Science Business Media B.V. 2014)
[49] *M. Lalanne, P. Berthier, J. Der Hagopian.* Mechanical Vibrations for Engineers (John Wiley and Sons, Chichester, New York, Brisbane, Toronto, Singapore 1984).
[50] *C.W. de Silva, Vibration and Shock Handbook.* (Taylor & Francis Group, Boca Raton, London, New York, Singapore, 2005).
[51] *E.J. Vernon - Carter, G. Avila de la Rosa, H. Carrillo Navas, Y. Carrera, J. Alvarez – Ramirez.* J. Food Engin.69, 18 (2016).
[52] *L.P. Gor'kov, and George Grüner (ed.).* Charge Density Waves in Solids (Modern Problems in Condenced Matter Sciences, vol. 25, Elsevier Science Publishers B.V., Amsterdam, Oxford, New York, Tokyo, 1989)
[53] *G.X. Tessema and N.P. Ong.* Phys. Rev. B. 31, 1055 (1985); Phys. Rev. B. 27, 1417 (1983).
[54] *R. Blinc, and A. P. Levanyuk (ed.).* Incommensurate Phases in Dielectrics, Part 1, Fundamentals; Incommensurate Phases in Dielectrics, Part II, Materials (Amsterdam North-Holland, 1986).
[55] *H.Z. Cummins.* Phys. Reports 185, 409 (1990).

Recevied: 12.06.2017